Agricultural and Forest Meteorology 225 (2016) 1–7

Contents lists available at ScienceDirect

Agricultural and Forest Meteorology

journal homepage: www.elsevier.com/locate/agrformet

Refining an inverse dispersion method to quantify gas sources on rolling terrain

Nan Hu[a,*], T.K. Flesch[a], J.D. Wilson[a], V.S. Baron[b], J.A. Basarab[c]

[a] Department of Earth & Atmospheric Sciences, University of Alberta, Edmonton, Alberta, Canada
[b] Agriculture and Agri-Food Canada, Lacombe, Alberta, Canada
[c] Alberta Agriculture and Rural Development, Lacombe, Alberta, Canada

ARTICLE INFO

Article history:
Received 18 September 2015
Received in revised form 18 April 2016
Accepted 5 May 2016
Available online 19 May 2016

Keywords:
Agricultural gas emissions
Flux measurements
Greenhouse gas emissions
Inverse dispersion
Wind variation over rolling terrain

ABSTRACT

This paper analyses a trace gas dispersion experiment with multiple point sources and line-averaging laser gas detectors on gently rolling terrain. The objective of the experiment was to establish how well emission rate can be inferred by "inverse dispersion" (ID), using a Lagrangian stochastic wind transport model (WindTrax) that (strictly) is appropriate only in horizontally-homogeneous winds. Measured mean wind speeds at fixed height above ground revealed spatial variation of order ±10% over the site. However the results of the inversion to estimate source strength Q from the concentration field suggest that the unwanted impact of the terrain is adequately compensated by representing detector light paths as curves, approximating their true height above ground. Under that treatment the mean and standard deviation of the ratio Q_{IDM}/Q of inferred to true source strength, over an ensemble of 96 fifteen minute intervals, were respectively $\langle Q_{IDM}/Q\rangle$=1.04 and $\sigma_{Q|Q}$ = 0.15, with little distinction between outcomes under unstable and stable stratification. We also used the measurements to study the influence (on the accuracy of retrieved source strength) of discretionary elements of inverse dispersion procedure: data quality criteria; optimal placement of detectors relative to the source(s); and the impact of alternative spatial representations of the source, supposing one had but *partial* information in that regard. Because the sources were always rather close to the downwind detector, the quality of the inversions was less sensitive to extremes of stratification than has been reported for other trials. Inversions that treated the actual point sources as an aggregate area source proved acceptable, provided this was placed at or near the height of the (true) point sources. An idealized distribution of elevated point sources can also be satisfactory, but bad inversions may result if placement of the token sources is biased in the cross-plot direction relative to the actual source(s).

1. Introduction

This paper is concerned with the practicability of measuring gas exchange between small surface sources and the atmosphere by inverse dispersion (Wilson et al., 2012), specifically under the circumstance that an assumption of uniformity (horizontal-homogeneity) of the wind field cannot strictly be justified, and/or the spatial distribution of the source or sources is only partially determined. Though this does not restrict the generality of our findings, the context of the paper is the task of measuring agricultural gas emissions from some element of a farm such as a single paddock, or a group of confined animals or a waste lagoon; such types of measurements spurred the work, and the analysis of a trace gas dispersion experiment from point sources over gently rolling terrain will be central to what follows.

It is well known that vertical flux measurements by eddy covariance or by the flux-gradient method are feasible only at sites satisfying certain practical limitations (Denmead, 1995; Foken, 2008; Aubinet et al., 2012). For instance the flow itself needs to be (nominally, and in the statistical sense) horizontally uniform, in order that the needed assumption of a vanishingly small mean vertical velocity be justifiable; and the source needs to be sufficiently extensive as to generate a constant flux layer of the gas in question (equivalently, the flux footprint must not extend off the source). In addition eddy covariance requires the existence of a suitably rapid gas detector, while a flux-gradient method demands that small mean concentration differences along the vertical can be determined with adequate accuracy.

* Corresponding author.
E-mail address: nhu1@ualberta.ca (N. Hu).

http://dx.doi.org/10.1016/j.agrformet.2016.05.007
0168-1923/

An inverse dispersion method (IDM) relaxes some of these requirements. Defined briefly, using IDM one measures the mean concentration of the target gas both upwind ("$\bar{c}_u$") and downwind ("$\bar{c}_d$") from the source, along with necessary meteorological information (for example the mean wind direction $\bar{\beta}$, the mean wind speed U at one height ("reference speed"), the Obuhov length L and aerodynamic roughness length z_0), and one invokes an atmospheric dispersion model to infer the emission rate Q necessary to "explain" the observed concentration rise ($\bar{c}_d - \bar{c}_u$). The model provides a *theoretical* value for the dimensionless "conversion number"

$$n = \frac{U(\bar{c}_d - \bar{c}_u)}{Q} \quad (1)$$

that takes into account the meteorological conditions and the known information – which may be complete or partial – regarding the particulars of the source and its placement relative to the detectors. The estimated flux Q_{IDM} is determined from the measured information ("meas") as

$$Q_{IDM} = \frac{[U(\bar{c}_d - \bar{c}_u)]^{meas}}{n} \quad (2)$$

and ideally $Q_{IDM}/Q = 1$ where Q is the true emission rate, in general unknown.

In suitable circumstances IDM is a convenient method with good accuracy. It is not restricted to large sources and, unlike some other possible techniques such as flux chambers, IDM is or can be a non-interfering method in that sensors can be placed out of the way of farm operations. As a rough guide, when IDM is implemented according to established guidelines (Flesch et al., 2004) it is found that individual 15- to 30-min determinations of Q typically scatter around the truth with a standard deviation of about 20% or less, and a bias of no more than about 5%. In the past decade many groups have estimated agricultural gas emissions using WindTrax,[1] which facilitates IDM to compute the theoretical conversion number (n) defined by Eq. (1). For further background please see Wilson et al. (2012).

Below we describe a trace gas dispersion experiment that was executed on rolling terrain, using continuous point sources of equal strength (in aggregate, "Q") and known location (these nominally simulated a herd of cows), and with line-averaged concentrations measured upwind and downwind. We analyse the accuracy of inverse dispersion estimates ("Q_{IDM}") of the true source strength Q in relation to assumptions or adjustments one might hypothetically invoke to compensate for, or minimize the negative impact of: (a) deviation of the wind statistics from Monin–Obukhov similarity theory (MOST) due to topography, and (b) incomplete information or erroneous assumptions about the spatial structure of the source.

2. Theory and methods

In what follows (u, v, w) are the wind velocity components along coordinates (x, y, z), where x is the east–west coordinate increasing towards the east and y the north–south coordinate increasing to the north. Reynolds decomposition splits the local, instantaneous value of u into its mean and fluctuation as $u = \bar{u} + u'$, etc.

2.1. Lagrangian stochastic trajectory model (WindTrax)

A flux measurement by inverse dispersion can be based on any appropriate dispersion model. Lagrangian stochastic (LS) trajectory models compute the $\bar{c} - Q$ relationship (i.e. the conversion number n needed for use in Eq. (2)) by computing an ensemble of N_P representative turbulent trajectories connecting the detector and the source. For simplicity, and as here, it is usually assumed that wind statistics obey MOST, and specialized software (e.g. WindTrax) has been developed to facilitate inverse dispersion using "MO-LS." Numerous groups have applied MO-LS to deduce emissions from various sources, often in an agricultural or waste management context. Examples include emissions of ammonia or methane from barns (Harper et al., 2010), from fields (Sanz et al., 2010), from waste storage ponds (Flesch et al., 2013), from feeder cattle (Todd et al., 2011), from beef cattle (Laubach et al., 2008) and from grazing cattle (McGinn et al., 2011).

WindTrax adopts the LS model given by Thomson (1987) for vertically-inhomogeneous Gaussian turbulence (i.e. the probability density function for velocity is assumed to be Gaussian), a common choice for the atmospheric surface layer. Needed Eulerian quantities are the mean horizontal velocity components $(\bar{u}, \bar{v})$; the turbulent velocity variances $(\sigma_u^2, \sigma_v^2, \sigma_w^2)$; the velocity fluctuation covariances $(\overline{u'v'}, \overline{u'w'}, \overline{v'w'})$; the turbulent kinetic energy dissipation rate (ε); and the surface roughness length z_0. With the assumption that MOST applies, measurements from a single sonic anemometer yield this needed information.

In the discussion below, wherever the inversion from observed concentration to inferred gas release rate has treated the source as a collection of *point* sources, $N_P = 5000$ trajectories were calculated forward from each source to the detector (i.e. WindTrax was used in forward mode). If the source was represented as an *area* source, however, backward mode was used with $N_P = 25{,}000$. These choices of N_P ensured that stochastic uncertainty in Q_{IDM} is negligible.

2.2. Site and equipment

In preparation for an inverse dispersion campaign to measure methane emissions from cattle, a tracer dispersion experiment was performed during August 2013 in "plot 22" at the Lacombe Research Centre (Agriculture and Agri-Food Canada, 52.457393 N, 113.765297 W). The topography and instrument layout at the site are indicated by Figs. 1–3; contours in Fig. (3) were derived from digital elevation files covering the township (TWP 40, ranges 27 and 26 west of the 4th meridian) that were purchased from AltaLIS ("LiDAR15 DEM", post spacing 15 m, vertical resolution 0.3 m). The mean roughness length at the site was about 0.08 m. The origin of the coordinate system used for WindTrax simulations coincides with the post in the SW corner of plot 22.

Eight point sources of tracer methane were distributed at known positions, within an overall area of about 20 m × 120 m (Fig. 2), in the gently rolling pasture. The distribution of the sources within a long, narrow area echoed the intended design for the eventual work with cattle, which was to ensure that for almost all mean wind directions $\bar{\beta}$ there should be markedly different upwind and downwind concentrations, despite the inevitable short term fluctuations of wind direction about the mean. The point of the tracer experiment was to evaluate the accuracy with which the inverse dispersion method would estimate the (in this case, known) emission rate Q, without accounting for any disturbance to the surface layer flow over the site: that is, WindTrax would be applied as if the terrain were perfectly flat and uniform, with the trajectory model driven by single point velocity statistics supplied by a sonic anemometer (Campbell Scientific CSAT3, operating at height $z = 1.97$ m), those statistics being height-extrapolated using Monin–Obukhov similarity theory. A set of matched cup anemometers measured the degree of spatial variation of the wind (see Section 2.3), but those data were not used in any way for the inversion of $(\bar{c}_u - \bar{c}_d)$ to obtain Q_{IDM}.

[1] "WindTrax" is a free software package written by B. Crenna that encodes forward and backward Lagrangian stochastic (LS) models into a graphical user interface (GUI), facilitating the application of the inverse dispersion method for small sources. It is applicable on the micrometeorological scale, and assumes the state of the surface layer is described by Monin–Obukhov similarity theory.

Fig. 1. A view of "plot 22" looking towards the north from the southern boundary fence. The origin of the coordinate system lies at the junction of the two visible fences, just out of sight at the lower left of the photograph. The light path of the laser gas detector at lower left runs northward, parallel to the fence defining the western boundary of plot 22, to a reflector seen just below the skyline. Also visible: cup anemometers, elevated gas release points, and a sonic anemometer at the right of the photo. The distance along the western fence from the origin to the gate on the skyline is 290 m.

The tracer methane was released from a cylinder at a rate that was controlled by a flow regulator, and flowed along equal-lengthed lines to the release points at height $h_{src} = 0.8$ m AGL (above ground level). As a backup check, cylinders were weighed before and after their contents had been consumed. Release rate was controlled at 0.97 kg h^{-1} (from 16th to 18th August) or 0.73 kg h^{-1} (21st and 22nd August). During suitable winds, gas was released continuously and measurements were aggregated to form 15 minute averages. A total of $N = 107$ such intervals were available for analysis, with $N_u^* = 77$ during unstable stratification ($-616 \le L \le -1$ m) and $N_s^* = 30$ under stable stratification ($+1 \le L \le +381$ m). However the run selection criteria that were eventually adopted (see Section 3.1) resulted in elimination of eleven of these runs, with the result that $N_u = 70$ and $N_s = 26$ runs were available for unstable and stable stratification, respectively.

The needed upwind and downwind concentration measurements were made using line-averaging laser gas detectors (Boreal Laser Gasfinder 2), one detector ("C39") running north–south on the west side and another ("C15") on the east side of the source distribution, with path lengths of 110 m. Fig. (2) is a schematic of the layout, and it should be evident that the distribution of the sources along the long axis (y) of the plot would have negligible impact on the line-averaged concentrations sensed by the laser detectors (this being a key attribute of the experimental design). Because of the rolling topography $h = h(x, y)$, the height $z'(x, y) = z - h(x, y)$ of the laser beams above the ground varied along the light path and differed for the two lasers. To obtain an approximate representation of $z'(x, y)$ for each path we sighted a vertical measuring rod, using a telescope mounted on top of the laser.

2.3. Inhomogeneity of the mean wind field

To ascertain the degree of inhomogeneity of the wind field at the site, mean wind speeds were measured by cup anemometers (Climet 011-4) at twelve locations (height $z = 1.12$ m AGL) distributed around the trace gas sources at the locations indicated in Fig. (3). Individual fifteen minute mean speeds were normalized relative to the value at one location (the reference location "ref", not far from the middle of the array of point sources), and these normalized mean speeds were binned (averaged) within sectors ($\bar{\beta} = \beta_0 \pm 22.5^\circ$) of mean wind direction centred on the cardinal directions $\beta_0 = 45, 90, \ldots 315^\circ$; mean wind direction $\bar{\beta}$ at a single point in the array was assumed to characterize the overall orientation of the flow. Then for each wind direction sector a mean relative windspeed was defined by averaging over all (270) runs for which mean windspeed at the reference location exceeded 2.5 m s^{-1}, this threshold being chosen to ensure any period during which cups may have stalled would not be included in the averaging.

Fig. (3) indicates that relative to the reference point, relative mean wind speeds varied from as low as about 0.9 to as high as about 1.05, i.e. variations of mean wind speed from place to place over the terrain did not exceed about ±10%. In terms of interpretation, at cup #9 (northernmost on the main transect) which sat in a gulley, the increased mean wind speed for a SSE wind can be understood as being a channelling effect. A quantitative comparison of the relative windspeed data with a linearized numerical flow model has been undertaken, and if one excludes wind directions for which steep terrain lay upwind of the anemometer array then there was a fair quantitative accord (not shown here). Thus in terms of the *degree* of inhomogeneity of the flow, it can be stated with certainty that deviations of order 10% occurred. Whether or not comparable changes occurred in higher order wind statistics, e.g. the standard deviation σ_w of the vertical velocity (which would exert a strong influence on the rate of vertical dispersion of plumes off the gas sources), is a matter of conjecture.

2.4. Representation of detector light paths

The light path of a line-averaging gas detector can be decomposed as a set of shorter line segments, or nominal "point" gas detectors, and each of those can be assigned an individual height z' above local ground. Even though the observed spatial variation of the mean wind speeds (at fixed height above ground) disapproved any thought that wind statistics in (x, y, z')-space might be horizontally homogeneous, it was of interest – as perhaps the optimal choice under the circumstances – to represent each detector path *as if* that were the case, transforming the straight laser light paths of (x, y, z)-space into curved light paths in (x, y, z')-space (Fig. 4).

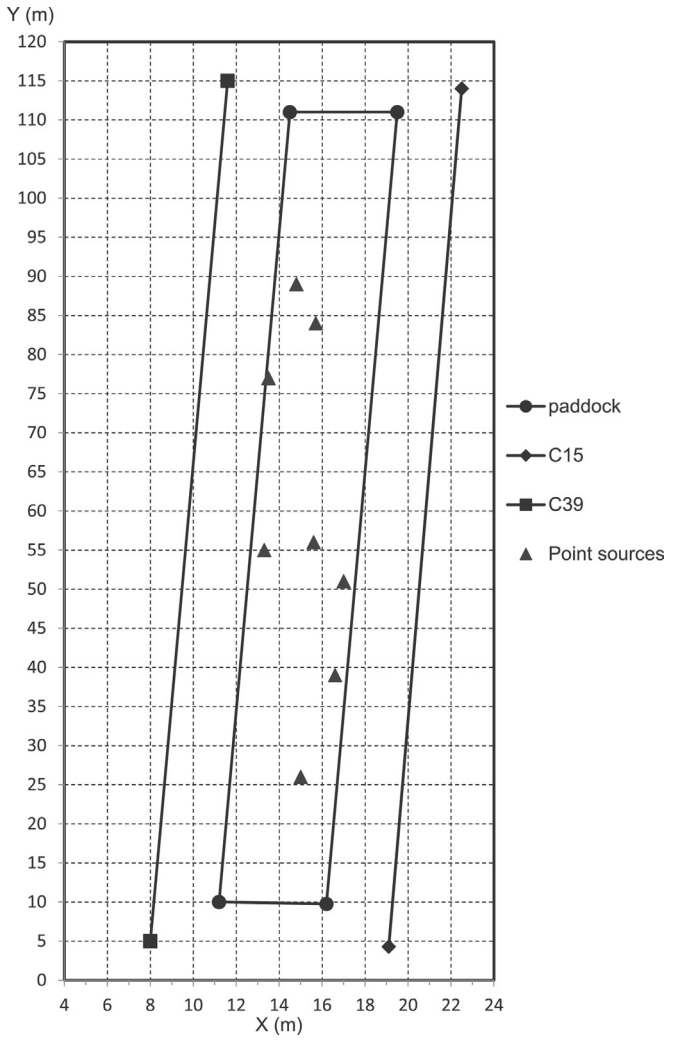

Fig. 2. Sketch of plot 22. For some inversions the trace gas source was represented as an effective *area* source bounded by the edges of the quadrilateral "paddock," whose corners are marked by the solid circles. The light path of detector C39 spans $(x, y) = (8, 5)$ to $(11, 115)$ m, while the light path of detector C15 spans (19, 4) to (23, 114) m.

This adjustment was carried out with a step length of 5.8 m along the beam, yielding 20 "point" detectors,[2] and we refer to this as representation **A**.

But that approach recommends itself only in the case that – as here – the true source location(s) are known. Therefore two simpler specifications that assign a *constant* light path height were also tested, namely:

B. The average of the beam height above ground sampled every 20 m from the south end of the paddock ($y = 5$ m) to the north end ($y = 105$ m), yielding $\bar{z'_{C39}} = 1.40$ m and $\bar{z'_{C15}} = 1.30$ m,
C. The average of detector height above ground and reflector height above ground, yielding $\bar{z'_{C39}} = 1.43$ m and $\bar{z'_{C15}} = 1.65$ m.

[2] Computational particles can be released from a point, but can never thereafter be located "at" a point. Therefore for forward simulations each "point" detector was of necessity treated as a volume, defined by a small cross-section running 5.8 m along the beam.

3. Results

Accuracy of the inversion can be gauged by statistics of the ratio Q_{IDM}/Q of inferred-to-true source strength, in a sample that includes many individual runs. The difference of the mean value $\langle Q_{IDM}/Q \rangle$ from unity is the "bias," while the standard deviation ("$\sigma_{Q|Q}$") is a measure of variability about that mean.

3.1. Sensitivity to filtering criteria

In the practice of inverse dispersion it is usual to exclude measurements stemming from intervals of extreme thermal stratification, or during which the distinction "upwind" versus "downwind" is meaningless: criteria on roughness length, wind direction, friction velocity and Obukhov length are usually used and cited. The impact of each of those filtering criteria is assessed below when implemented alone (i.e. without any other filtering), and with the detector beams represented as curved light paths in (x, y, z')-space (the terrain following coordinate, specification **A**).

3.1.1. Surface roughness length

Four alternative ensembles of runs were defined, by eliminating runs for which the roughness length[3] exceeded an upper threshold value z_0^{thres} set variously as $z_0^{thres} = (0.05, 0.1, 0.15, 0.25)$ m. Across these ensembles the mean performance as defined by $\langle Q_{IDM}/Q \rangle$ varied without regularity from approximately 1.08 to 1.09, and there was (likewise) no pattern in $\sigma_{Q|Q}$. Therefore in the following analysis no data were rejected on the basis of the roughness length.

3.1.2. Mean wind direction

Based on the geometry of the experiment, it was evident that the point detectors would not detect a meaningful concentration difference whenever the wind blew nearly parallel to the long axis of the plot, i.e. from the north or from the south. If observations were rejected for periods of northerly or southerly winds by rejecting data for which $\bar{\beta}$ lay within sectors spanning $\pm 30^\circ$ or $\pm 20^\circ$ or $\pm 10^\circ$ about due north (or south), the mean ratio over all retained intervals improved markedly from $\langle Q_{IDM}/Q \rangle = 1.09$ (no filtering based on mean wind direction) to $\langle Q_{IDM}/Q \rangle = (1.04, 1.04, 1.04)$ respectively, while the standard deviation decreased from $\sigma_{Q|Q} = 0.33$ (with no filtering based on mean wind direction) to $\sigma_{Q|Q} = (0.12, 0.13, 0.15)$ respectively. Thus rejection sectors spanning $\pm 10^\circ$ about $0/360^\circ$ and 180° were adopted, and suffice to filter out periods having an ambiguous wind direction.

3.1.3. Friction velocity and Obukhov length

Fig. (5) summarizes the performance of inverse dispersion (as characterized by $\langle Q_{IDM}/Q \rangle$) for different combinations of u_* and $|L|$ rejection thresholds, the leftmost column corresponding to $|L| \geq 0$ (i.e. no filtering whatsoever in regard to L). If data are rejected for intervals having friction velocity below a threshold value $u_*^{thres} = (0.05, 0.1, 0.15)$ m s^{-1} the mean performance improved slightly from $\langle Q_{IDM}/Q \rangle \approx 1.05$ (no threshold) to $\langle Q_{IDM}/Q \rangle \approx (1.04, 1.03, 1.02)$, while the standard deviation remained constant at $\sigma_{Q|Q} \approx 0.12$.

Earlier tests (Flesch et al., 2004) have reported a small improvement in the accuracy of the inverse dispersion method when a threshold magnitude L^{thres} for the Obukhov length is imposed (i.e. runs are rejected when $|L| < L^{thres}$). In the present experiment such

[3] The apparent roughness length for each interval was diagnosed from data provided by the sonic anemometer, specifically the mean horizontal wind speed, the magnitude u_*^2 of the kinematic vertical momentum flux density, and the kinematic virtual heat flux density $\overline{w'T'_v}$. By optimization of the roughness length z_0 (treated as flexible, run by run) these data were required to conform to the Monin–Obukhov mean wind profile.

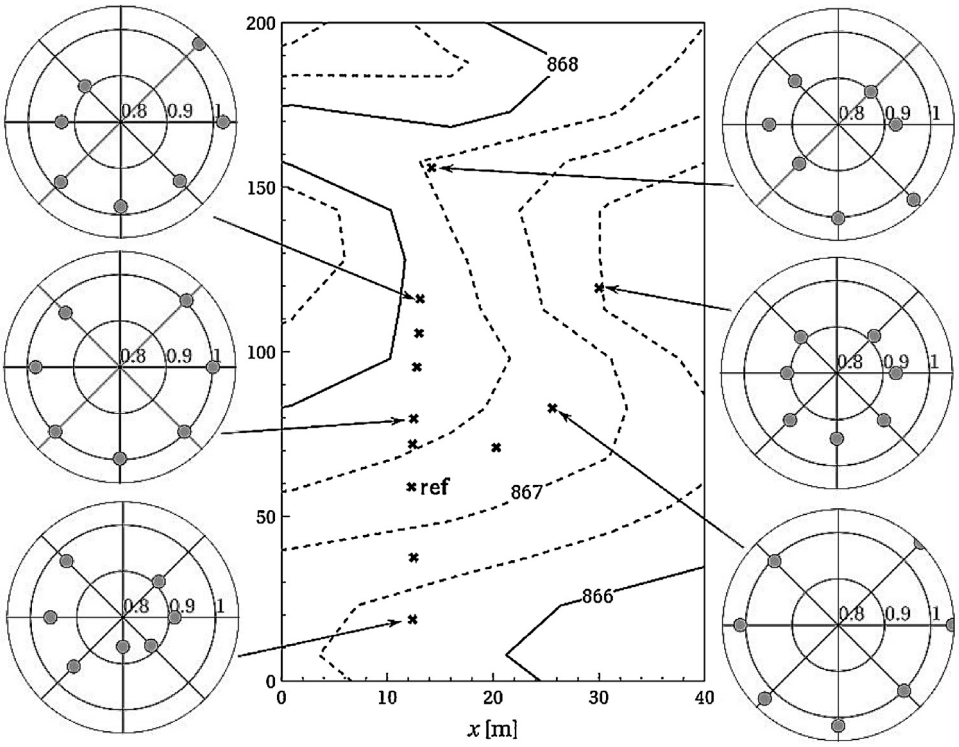

Fig. 3. A view of the terrain (contour elevations in m above sea level), with positions of cup anemometers (crosses) and some of the associated wind roses. Wind rose gives the mean relative wind speed within each wind direction sector, e.g. $90 \pm 22.5^{\circ}$. The reference anemometer is denoted "ref". The relative windspeed axis spans the range 0.8–1.05. Winds from the *N* sector did not occur during the experiment.

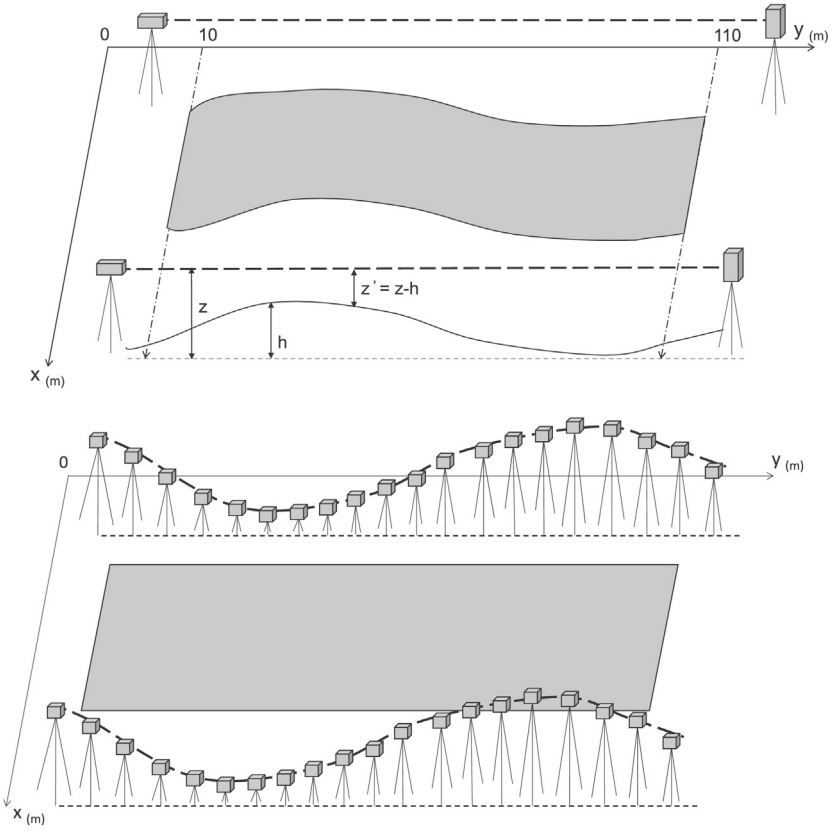

Fig. 4. Upper panel: definition of terrain following coordinate for detector height. Lower panel: detector light paths, curved after adopting terrain following coordinate.

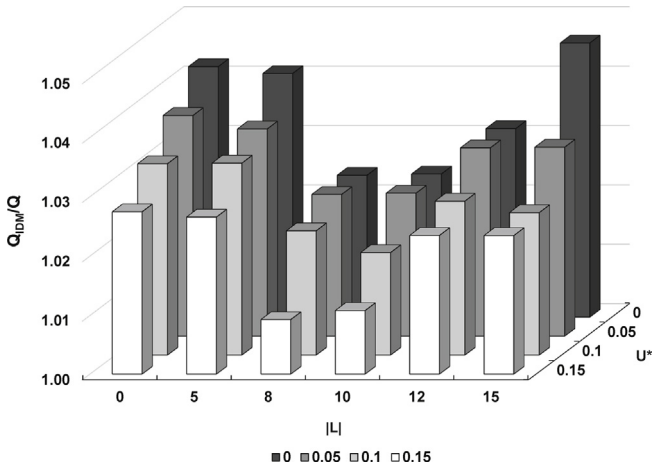

Fig. 5. Mean performance $\langle Q_{IDM}/Q \rangle$ of the inverse dispersion method in relation to the imposition of filtering based on imposed *minimum values* for the magnitude $|L|$ [m] of the Obukhov length and for the friction velocity u_* [m s^{-1}]. The leftmost column corresponds to $|L| \geq 0$ (i.e. no filtering in regard to L), while the rear (black) row corresponds to $u_* \geq 0$ (i.e. no filtering in regard to u_*).

a filter did not result in a convincing improvement in the accuracy of the inversion for Q_{IDM}, for while the bias and scatter do decrease when runs having $|L| < 8$ m are rejected, such that $\langle Q_{IDM}/Q \rangle$ falls from about 1.04 to 1.02 and $\sigma_{Q|Q}$ from around 0.16 to 0.12, the bias increases again so soon as a larger threshold magnitude is imposed. Of course the pattern shown in Fig. (5) may reflect idiosyncrasies of the data, i.e. the retention or rejection of a given run having Q_{IDM}/Q very different from unity can explain the irregularity of the pattern.

From Fig. (2) it is obvious that in this experiment, excluding intervals of very oblique winds (i.e. periods of small $\bar{\beta} - 0^\circ$ and small $\bar{\beta} - 180^\circ$), the distance from the sources to the downwind detector was small and thus the detected plumes would normally have been shallow. Given that the influence of stratification is diminished at small $|z/L|$, it is perhaps understandable that filtering relative to L had little impact. In short, for the inversions upon which further results are based there is *no filtering* with respect to the magnitudes of (u_*, L).

Accordingly, a single filtering criterion, based on mean wind direction alone, applies across the results to follow. The resulting set of 15-min intervals contained $N_u = 70$ runs under unstable stratification (spanning $-616 \leq L \leq -3.1$ m) and $N_s = 26$ under stable stratification (spanning $2.2 \leq L \leq 381$ m). One final (and subjective) element merits mention: it can be seen from Eqs. (1 and 2) that if the conversion number n is tiny or vanishes (negligible or zero concentration rise, according to the model) then the inverse dispersion procedure returns a large or infinite source strength Q_{IDM}. We felt it legitimate and necessary to remove those cases, for otherwise statistics of the ensemble of inversions would have been useless. Happily only two observation periods (of the 96 otherwise accepted) gave extreme outliers – and at that, only for one particular configuration for the inversion, in which the modelled plume passed beneath the downwind laser.

3.2. Effect of representation of detector beams

Table 1 summarizes the outcomes for each of the three representations of the detector light paths. With choice A (the terrain following coordinate) the inversion gives $\langle Q_{IDM}/Q \rangle$=1.04 and $\sigma_{Q|Q} = 0.15$. Using specifications B and C, the mean ratios are $\langle Q_{IDM}/Q \rangle$ = (1.04, 1.59) and the standard deviations $\sigma_{Q|Q}$ = (0.17, 0.88) respectively. We conclude that compensating for the variable (actual) height of the detector beams above ground improves accuracy, and that by a small margin practice **A** (the terrain following coordinate) is best. The relative merits of practices **A** and **B** may well hinge on particularities, and differ in other experiments.

Table 1
Performance of inverse dispersion given the true positions of the eight point sources: mean $\langle Q_{IDM}/Q \rangle$ and standard deviation $\sigma_{Q|Q}$ (in brackets) of the ratio Q_{IDM}/Q, for each representation (**A**, **B** or **C**) of the height of the detector light paths.

# Runs	Span in L [m]	Practice **A** Terrain following	Practice **B** Avg.	Practice **C** Avg. src &dtctr
70	$-616 \leq L \leq -3.1$	1.03 (0.16)	1.02 (0.17)	1.46 (0.34)
26	$2.2 \leq L \leq 381$	1.06 (0.14)	1.11 (0.14)	1.96 (1.55)
96	$-616 \leq L \leq 381$	1.04 (0.15)	1.04 (0.17)	1.59 (0.87)

Table 2
Performance of inverse dispersion versus one's adopted representation of the source distribution and detector beam height (**A** or **B**). Each group of numbers gives: the mean $\langle Q_{IDM}/Q \rangle$ and standard deviation ($\sigma_{Q|Q}$, in brackets) of the ratio Q_{IDM}/Q, and (if specified) the count N of contributing inversions (where not specified, N = 95 or 96).

Assumed source configuration	Practice **A** Terrain following	Practice **B** Avg., $\Delta y = 20$ m
Area source on surface	1.76 (1.05)	1.32 (2.42)
Area source ($z = 0.8$ m)	1.09 (0.23)	1.03 (0.21)
Point sources ($z = 0.8$ m)		
(a) Along centreline	1.06 (0.15)	1.03 (0.15)
(b) Randomly placed	1.06 (0.17)	1.05 (0.16)
(c) Along E edge, E winds	1.85 (1.02) 33	1.62 (0.64) 33
W winds	0.89 (0.20) 63	0.92 (0.39) 63
True distribution (as in Table 1)	1.04 (0.15)	1.04 (0.17)

3.3. Alternative representations of the source

For the results given above, the detected concentration signals were inverted with the à priori knowledge that the concentration field had been caused by eight point sources of equal strength and all the same height ($h_{src} = 0.8$ m), these being irregularly distributed but at known positions. Recall too, that the actual distribution of the sources along the y-axis has no impact on the line-averaged concentrations detected by the lasers.

But supposing one did not know the source distribution: how should the source best be represented? Are some assumptions liable to be safer than others? In general, two broad options apply, i.e. representation as an area source, or as a collection of point sources. For each manner of representing the source, we tested the strategies **A** and **B** in regard to representation of the detector beams.

3.3.1. Area source treatments

Since (in the sorts of applications envisaged) the animals would be fenced into a paddock, we tested the assumption of an area source with known perimeter (the "paddock" shown in Fig. 2), located either on ground, or at an elevation of $h_{src} = 0.8$ m (same as the release height of the actual point sources, which corresponds roughly to the release height of the breath of an animal).

Table 2 gives the values of $\langle Q_{IDM}/Q \rangle$ for the area source treatments investigated. If emission is assumed to occur at the ground surface the outcomes of strategies **A** and **B** are both poor, with $\langle Q_{IDM}/Q \rangle$=1.76, 1.32 and $\sigma_{Q|Q} = 1.05, 2.42$. On the other hand if the area source is assumed to be elevated, and provided filtering based on mean wind direction was applied, specifications **A** and **B** resulted in satisfactory inversions with $\langle Q_{IDM}/Q \rangle$=1.09, 1.03 respectively, along with tolerably small standard deviations $\sigma_{Q|Q} = 0.23, 0.21$.

3.3.2. Point source treatments

We studied three assumed spatial distributions of the eight point sources that (in all cases) were elevated at height $h_{src} = 0.8$ m above the surface; and once again, each configuration was analysed using strategies **A** and **B** for representing detector beam height.

The sources were alternatively (**a**) spaced along the centre line of the paddock, spanning its long axis; (**b**) distributed randomly over the paddock (but with a uniform distribution along the x-axis); and (**c**) spaced along the east edge of the "paddock" (see Fig. 2). Note that for distribution **c** the fetch from the sources to the downwind detector is at a minimum for west winds and at a maximum for east winds. One therefore expects a dichotomy in the outcome of **c** depending on the wind direction – underprediction of the emission rate during westerly winds and overprediction during easterly winds – and so we segregate the outcomes for distribution **c** for easterly ($\bar{\beta} = 90 \pm 80^\circ$) and westerly ($\bar{\beta} = 270 \pm 80^\circ$) winds.

The results of applying strategies **A** and **B** to point sources spaced along a centre line were respectively $\langle Q_{IDM}/Q \rangle = (1.06, 1.03)$ (Table 2), and rather similar outcomes are obtained by assuming randomly distributed point sources: $\langle Q_{IDM}/Q \rangle = (1.06, 1.05)$. However if the point sources are assumed to be distributed on the extremity of the paddock, the outcomes are much inferior: for easterly winds $\langle Q_{IDM}/Q \rangle = (1.85, 1.62)$, while for westerly winds $\langle Q_{IDM}/Q \rangle = (0.89, 0.92)$. What we conclude from distribution **c** is that, unsurprisingly, there is a loss of accuracy if the assumed source location is biased (in the cross-plot direction) relative to the actual distribution.

4. Discussion and conclusion

The tracer experiment described above was intended to map out the feasibility of applying inverse dispersion to determine methane emission rate from a small herd of cows (circa 10 animals), loosely confined in a long narrow paddock, but without knowledge of actual animal positions. Recall that by virtue of use of the line integrating detectors, and if it were true that wind statistics were horizontally-homogeneous, only the x-coordinate or "cross-plot" position of a source can affect the inversion.

In terms of filtering criteria to weed out intervals unsuitable for inverse dispersion analysis, we found that the most important step is to eliminate periods with unsuitable mean wind direction: for the geometry of our tracer experiment, removing periods for which $\bar{\beta} = 0 \pm 10^\circ$ or $180 \pm 10^\circ$ is a satisfactory compromise. Further filtering, i.e. imposition of criteria on the friction velocity and Obukhov length, proved of little advantage – in agreement with the findings of Flesch et al. (2014).

If uncertainty as to 'animal' position is eliminated, then despite the departure of the experimental site from the ideal of flat, uniform terrain, standard MO-based inverse dispersion using WindTrax yielded a very satisfactory estimate of aggregate source strength ($\langle Q_{IDM}/Q \rangle$=1.04, $\sigma_{Q/Q} < 0.2$), and this regardless of whether one treated the detector as a curved light path at actual beam-height-above ground, or assumed a constant path height equal to the average path height alongside the paddock (these figures are very comparable with those observed in similar tracer experiments on truly flat terrain, rather to our surprise). Furthermore with the (true) source distribution of these tracer trials, which mimicked eight 'cattle' spread out over the paddock so that their cross-plot distribution was not biased towards either side of the paddock, the accuracy of the inversion (with detector representations **A** or **B**) was not very sensitive to one's spatial representation (in the inversion) of the effective source: excellent accuracy was obtained ($\langle Q_{IDM}/Q \rangle = 1.03$–$1.09$) regardless of whether the tracer source was represented using the eight actual positions, or using eight sources evenly or randomly distributed across the paddock, or by way of a single elevated area source.

There are however two concerns with the design. First is the sensitivity to assumed source height, for while the inversion yields good accuracy in $\langle Q_{IDM}/Q \rangle$ when the true source height is used (e.g., area source at height $h_{src} = 0.8$ m) the outcome is poor (see Table 2) if that area source is placed on ground (a consequence of the close proximity of the downwind detector to the source). When measuring enteric emissions (from the breath) the mouth height of the cattle is unlikely to be known with accuracy, and this sensitivity to source height is undesirable. The second concern is the error that would result if cattle congregated systematically on one side of the paddock, for calculations (not shown) indicate a bias of up to a factor of two in the estimated emission rate. A sensitivity study using WindTrax showed that this potential bias would be less serious were the laser paths to be placed further from the paddock boundaries, reducing the fractional uncertainty in upwind fetch to the source(s) and lessening sensitivity of the conversion number n to the uncertain release height.[4] As an anonymous reviewer remarked, sensitivity trials using a dispersion model (such as WindTrax) are helpful, indeed virtually essential, in designing an experiment and in assessing what degree of uncertainty might attach to results.

Acknowledgments

This research has been funded by a grant from the Agricultural Greenhouse Gases Program of Agriculture and Agrifood Canada, and by the Natural Sciences and Engineering Research Council of Canada. The authors acknowledge the assistance of Peter Carlson (Dept. Earth & Atmospheric Sciences, University of Alberta) and David Young (Agriculture and Agri-Food Canada, Lacombe).

References

Aubinet, M., Vesala, T., Papale, D., 2012. Eddy Covariance: A Practical Guide to Measurement and Data Analysis. Springer Atmospheric Sciences, 438 pp. ISBN 978-94-007-2350-4.
Denmead, O.T., 1995. Novel meteorological methods for measuring trace gas fluxes. Philos. Trans. R. Soc. Lond. A 351, 383–396.
Flesch, T.K., Wilson, J.D., Harper, L.A., Crenna, B.P., Sharpe, R.R., 2004. Deducing ground-air emissions from observed trace gas concentrations: a field trial. J. Appl. Meteorol. 43, 487–502.
Flesch, T.K., Vergé, X.P.C., Desjardins, R.L., Worth, D., 2013. Methane emissions from a swine manure tank in western Canada. Can. J. Anim. Sci. 93, 159–169.
Flesch, T.K., McGinn, S.M., Chen, D., Wilson, J.D., Desjardins, R.L., 2014. Data filtering for inverse dispersion emission calculations. Agric. For. Meteorol. 198–199, 1–6.
Foken, T., 2008. Micro-meteorology. Springer, 306 pp. ISBN 978-3-540-74665-2.
Harper, L.A., Flesch, T.K., Wilson, J.D., 2010. Ammonia emissions from broiler production in the San Joaquin Valley. Poult. Sci. 89, 1802–1814.
Laubach, J., Kelliher, F.M., Knight, T.W., Clark, H., Molano, G., Cavanagh, A., 2008. Methane emissions from beef cattle: a comparison of paddock and animal-scale measurements. Aust. J. Exp. Agric. 48, 132–137.
McGinn, S.M., Turner, D., Tomkins, N., Charmley, E., Bishop-Hurley, G., Chen, D., 2011. Methane emissions from grazing cattle using point-source dispersion. J. Environ. Qual. 40, 22–27.
Sanz, A., Misselbrook, T., Sanz, M.J., Vallejo, A., 2010. Use of an inverse dispersion technique for estimating ammonia emission from surface-applied slurry. Atmos. Environ. 44, 999–1002.
Thomson, D.J., 1987. Criteria for the selection of stochastic models of particle trajectories in turbulent flows. J. Fluid Mech. 180, 529–556.
Todd, R.W., Cole, N.A., Rhoades, M.B., Parker, D.B., Casey, K.D., 2011. Daily, monthly, seasonal, and annual ammonia emissions from southern high plains cattle feedyards. J. Environ. Qual. 40, 1–6, http://dx.doi.org/10.2134/jeq2010.0307.
Wilson, J.D., Flesch, T.K., Crenna, B.P., 2012. Estimating surface-air gas fluxes by inverse dispersion using a backward Lagrangian stochastic trajectory model. In: Lagrangian Models of the Atmosphere. American Geophysical Union, Geophysical Monograph 200, pp. 149–161, 349 pp.

[4] Sensitivity of an inversion to uncertainty in the release height h_{src} should decay (with increasing downwind displacement of the concentration detector) roughly on length scale $h_{src}\,\bar{u}(h_{src})/\sigma_w(h_{src})$.